Models of cross shelf transport introduced by the Lofoten Maelstrom

A. Ommundsen*

Department of Mathematics, University of Oslo, P.O. Box 1053 Blindern, Oslo, Norway

Abstract

The drift of particles released in the tidal current (Moskstraumen) near Lofotodden, located at 67°50′N, 12°50′E, has been studied. The periodical tidal current combined with a background current is found to introduce a transport between Vestfjorden inside Lofotodden and the shelf outside. This particular transport may be important for the drift of cod eggs, larvae and other important biological and chemical tracers. A fine-resolution numerical model provided the Eulerian tidal current field based on which the particle trajectories are calculated using a Lagrangian particle tracking technique. The tracking algorithm was extended by a random-walk method to simulate small scale turbulence. An idealized current model of the area is also developed for use as a simplification tool to reveal the basic mechanisms of the drift and to demonstrate the sensibility of time stepping in numerical integration. © 2002 Elsevier Science Ltd. All rights reserved.

Keywords: Maelstrom; Particle motion; Shelf dynamics; Tidal currents; Water exchange

1. Introduction

To make scientific well judged decisions regarding the resources along the coast of Norway, better knowledge about how the tide influences the local ocean environments is needed. Periodic tidal variations in the ocean surface dominate other oceanographic signals, and the tidal currents will represent an important part of the overall current field. Tidal currents commonly of order 1 m/s may be significantly increased when constrained by topography. The famous tidal current Moskstraumen, also known as the Lofoten Maelstrom,

outside Lofotodden is an example, running with strength up to 3–5 m/s.

In an earlier work by Gjevik et al. (1997), a fine-resolution numerical model for the tide around Lofoten was developed. The domain of this model is depicted in Fig. 1. The article documented high difference in the sea level in the sound between Lofotodden and Værøy, with the small island Mosken in the middle (Fig. 1, right panel). The maximum strength of Moskstraumen was estimated to be approximately 3 m/s for the M_2 component. With the tidal current data from Gjevik et al. (1997) and idealized background currents (*BC*s), we have studied horizontal particle drift in Moskstraumen. The particle tracking algorithm in this report is similar to the method

*Tel.: +47-2285-5866; fax: +47-2285-4349.

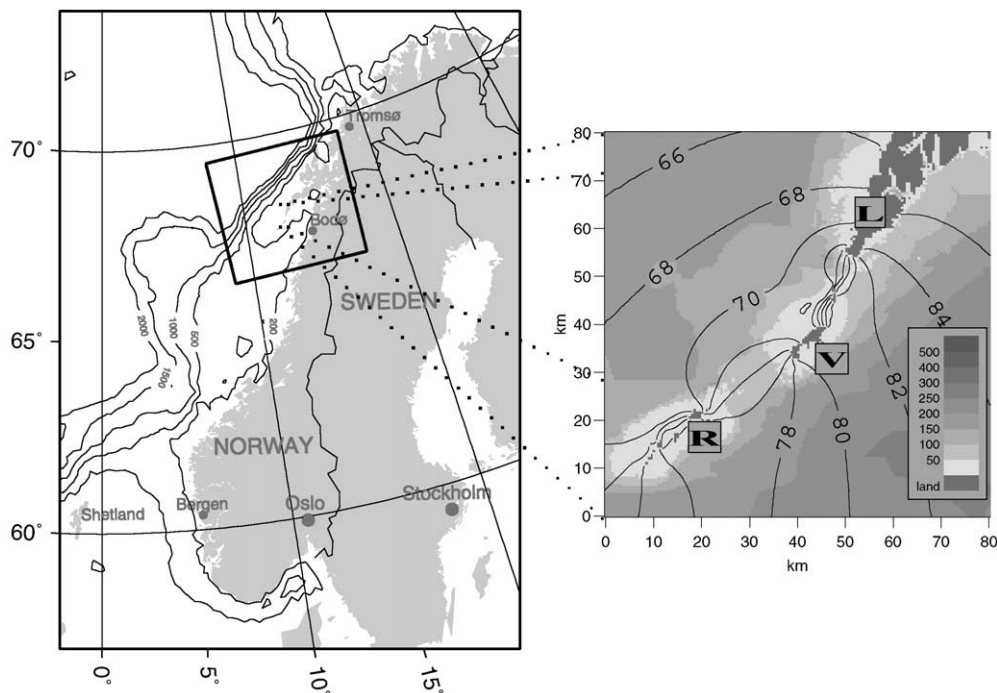*E-mail address:* atleo@math.uio.no (A. Ommundsen).

Fig. 1. Square box in left panel shows the location of Lofoten and the total model domain. Lofoten is located on the northern Norwegian continental shelf (left). Vestfjorden lies inside the Lofoten archipelago northwest of Bodø. Right panel: enlarged map of the area near Lofotodden. The labels are: Lofotodden (L); Værøy (V) and Røst (R). Color depth scale in meters (legend), and contour lines for amplitude with equidistant 2 cm for the M_2 tidal constituent.

used by Gjevik (1996) to simulate particles drift in the tidal flow in other regions along the Norwegian coast. The tide combined with the steady *BC* in the area is shown to be an important mechanism for exchanging water-masses between Vestfjorden and the open sea. Although this study primarily focuses on a particular application, similar mechanism for cross shelf transport can be important in other areas. The results of this study may therefore be of a wider interest.

Numerous papers concerning particle drift and dispersion in the ocean and atmosphere exist. In these papers, several solution methods are proposed. The paper by Turell (1994) reviews some of the numerical modeling efforts that took place during the days following the grounding of the tanker *Braer*. Several organizations participated in the development of numerical models predicting the oil spill, which was initially located at the tip of Shetland Island. These models were repeatedly compared to data. The conclusion was that forecasting movement of oil and water under action of tide and wind may be accomplished using computer models and the need for higher spatial resolution was stressed. Due to severe weather conditions, the necessary model parameters, derived from measurements at sea, were unreliable and difficult to obtain. This combined with the need to develop new or to improve existing numerical models during the propagation of the spill made forecasting unreliable.

The largest deliberate oil spill, 25 km south of Kuwait City in 1991, is modeled in the article by Proctor et al. (1994b). Controlled and legal releases of oil was made in the North Sea, and the observed drift was used to validate a numerical model discussed in Elliott et al. (1986) and Elliott (1986). These models used the Lagrangian particle tracking and the random-walk techniques instead

of the more classic advection–diffusion equation approach.

The importance of residual currents is discussed in the articles by Zimmerman (1986), Ridderinkhof and Zimmerman (1992) and Geyer and Signell (1992). A nonlinear tidal model will introduce residual currents which may exhibit considerable variability over the length of the tidal excursion (i.e. the horizontal displacement of fluid particles). This perturbation of the basic oscillatory flow can generate chaotic particle motions, in that particles released at nearby positions at a special moment follow strongly divergent pathways in later times.

In this report, the complex drift of particles released is due to gradients in the Eulerian current field and the net transport is caused by the interaction between the oscillatory tidal flow and the steady BC. The BC in the area is much larger than the tidal residual current, so in this study the latter was neglected. A random-walk algorithm was also implemented to simulate turbulence on small scale. The effect and reliability of this algorithm are strongly connected to the choice of diffusion coefficients. In Elliott et al. (1992), Elliott (1986) and Proctor et al. (1994b) the random-walk technique is used with different models for the diffusion coefficient.

The north-west part of Vestfjorden is an important spawning area for the Arcto-Norwegian cod during March and April (Ellertsen et al., 1980). Moskstraumen, combined with the general circulation, should therefore be an important actor in the transport of cod eggs, larvae, etc. between Vestfjorden and the open ocean. Simulations of particles studied in this report indicate horizontal drift and dispersion of zooplankton, eggs, pollution, etc. These quantities are treated as passive particles drifting with flow, assuming swimming and migration of minor importance.

2. Equation for particle motion

The high-resolution tidal model of Gjevik et al. (1997) and Moe et al. (accepted for publication) provides time series of currents and sea level with a spatial resolution of 500 m. These simulations are made with a depth-integrated linear model of the shallow water equation including gravity, Coriolis and quadratic bottom shear stress. Harmonic analysis is then performed on these time series to determine the amplitude and phase of the tidal components included in the model (M_2, N_2, S_2 and K_1). The simulations of Gjevik et al. (1997) and Moe et al. (accepted for publication) predict the M_2 current in Moskstraumen to be approximately 5–10 times stronger than the other semidiurnal or diurnal components. With a horizontal Cartesian coordinate system, origin at left lower corner and x-, y- axis along the model domain (Fig. 1), the x and y components of the M_2 depth mean current velocity are represented, respectively, as

$$u(x, y, t) = U \cos(\omega t + \chi - \delta_u), \tag{1}$$

$$v(x, y, t) = V \cos(\omega t + \chi - \delta_v). \tag{2}$$

Here, (U, V) denotes the amplitudes, ω the angular velocity, (δ_u, δ_v) the phases relative to Greenwich and χ the astronomical argument. The current field due to other tidal components may be included in expressions (1) and (2); see Gjevik (1996). With a nearly linear tidal model and approximations (1)–(2), we neglect the effect of tidal driven residual currents.

Lagrangian motion of particles is found by integrating the equations

$$\frac{\mathrm{d}x_k}{\mathrm{d}t} = u(x_k, y_k, t), \quad \frac{\mathrm{d}y_k}{\mathrm{d}t} = v(x_k, y_k, t). \tag{3}$$

Subscript k denotes the number of single particle ($k = 1, \ldots, M$, $M = $ number of particles) and (x_k, y_k) its position.

3. Numerical method and accuracy

We have used a fourth-order Runge–Kutta method as initiator combined with an Adams–Moulton method for the numerical integration of Eqs. (3). This combination will reduce the computer time, still keeping a truncation error of Δt^5 (e.g. Boyce and DiPrima, 1992).

In the idealized model, described in Section 4, the current is provided by an analytical formula and the current field is hence described for all

location in time and space. In the Lofoten model, however, described in Section 5, the data originate from a finite difference method and are therefore discontinuous. We therefore use a bilinear interpolation routine between four spatial grid points to generate the information needed in between the finite difference grid points. In each grid point, the current is continuous in time due to the representation given by Eqs. (1) and (2). The use of unmodified bilinear interpolation is a source to unwanted effects near land. Nearest-neighbor interpolation, which returns the value of the closest grid point, was therefore used if the nearest neighbor had zero velocity. Particles are "beached" when they encounter a dry grid cell. There are numerous ways to treat beached particles, e.g. Proctor et al. (1994a, b). In our simulations beached particles are deadlocked for the rest of the simulation.

Unreliable trajectories and even on-shore drift of particles is the consequence of using too large time step in the numerical integration. A sufficiently small enough time step ensures that no particles move more than a fraction of a grid cell in one time step. In these simulations, the convergence of the particle path with decreasing time step was used to find an appropriate time step, see discussion Section 4.1.

By solving Eqs. (3) we can simulate advection to a high degree of accuracy. The dispersion of a passive substance within such a fluid is not resolved by the advection alone. Turbulence will contribute to a random displacement of the particles released. The Lagrangian particle-tracking technique simulate turbulent diffusion effectively by the use of a 'random-walk' method (Hunter, 1987).

We define a diffusion length

$$D = R_1 \sqrt{12 K_h \Delta t}, \tag{4}$$

where R_1 is a random number drawn from a uniform distribution between 0 and 1 and K_h is the diffusion coefficient. The position of a particle was then calculated by numerical integration of Eqs. (3) combined with a displacement of length D each time step. The direction of the displacement D was set by the angle $2\pi R_2$, where R_2 is a random number also drawn from a uniform distribution between 0 and 1.

Homogeneous diffusion on a small scale is modeled by a constant diffusion coefficient K_h. This random method alone is then a simulator of the Fickian dispersion, where the corresponding effective diffusivity, K, is given by

$$K = \frac{1}{2} \frac{d\sigma^2}{dt}. \tag{5}$$

Here, σ^2 is the variance of the particle distribution calculated in any direction. The scaling of the diffusion length D combined with the direction of displacement $2\pi R_2$, provides a diffusion coefficient K_h which equals the effective diffusivity K. Eq. (5) can be obtained by investigating the mass (the zeroth moment), center of mass (the first moment) and the variance (the second moment) deduced from the diffusion equation. Furnes (1994) analyzed these moments and also demonstrated the close resemblance between the solution of the random method and the diffusion equation for available analytical solutions of the diffusion equation. With a constant diffusion, the center of mass will not change in time and the variance is proportional to the diffusion. A gradient in the diffusion will cause the centroid to move in the direction of stronger diffusivity. Results with the diffusion term active are provided in Section 6.

4. An idealized model

It is of interest to first study particle motion in an idealized model. This idealized model captures important dynamics of the current field near Lofotodden. Such a model enables a more controllable model environment, and reveals the basic mechanism for the exchange between Vestfjorden and the outer shelf.

The model geometry is shown in Fig. 2. The model domain consists of two impenetrable walls, representing, respectively, Lofotodden and the island chain south of Værøy. Although the numerical model implements these walls with an infinitely small width, they are drawn with an artificial extension in the figures. An aperture of $b = 16$ km separate these walls, which is approxi-
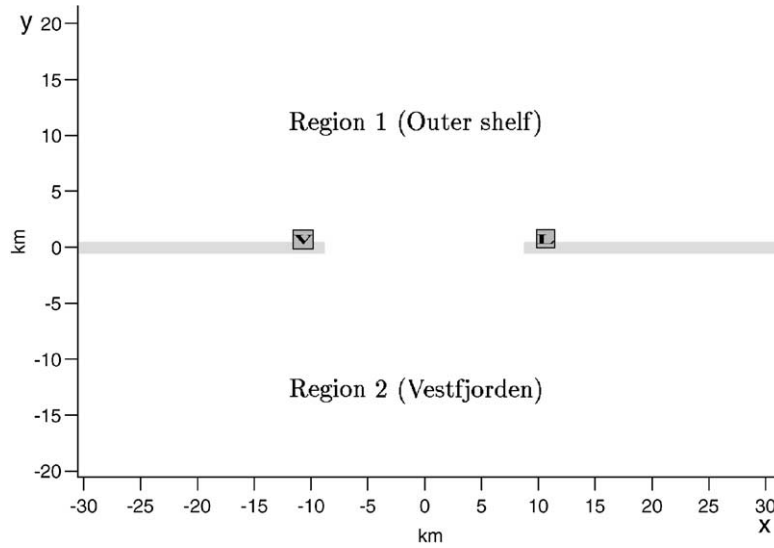
Fig. 2. Two solid, impenetrable walls represent, respectively, Værøy (V) and Lofotodden (L). The outer shelf is marked as region 1 ($y > 0$), while Vestfjorden is marked as region 2 ($y < 0$).

mately the true distance between Værøy and Lofotodden. In this simple model, these walls are infinite on both sides of the aperture.

Moskstraumen is simulated by a flow through an aperture (Milne-Thomson, 1968, p. 158). The equation for this flow is

$$\frac{x^2}{c^2 \cos^2(\alpha\psi)} - \frac{y^2}{c^2 \sin^2(\alpha\psi)} = 1. \tag{6}$$

Here, ψ denotes the stream function. Streamlines $\psi = $ constant are confocal hyperbolas, with foci $(-c, 0), (c, 0)$. The speed at these foci will be infinite, thus our aperture must be chosen $b < 2c$. We chose c to be 10 km and $b = 16$ km. Streamlines that intersect the x-axis outside our aperture ($|x| > 8$) are naturally excluded. The parameter α controls the strength of the current. The flow is multiplied with $\cos(2\pi/T\, t - \delta)$, $T = 12.4$ h, to provide the oscillation of the M_2 tidal current. The phase δ is included to control the initial direction and strength of this flow. The velocity profile between the coordinates ($\pm 8, 0$) is a parabola with maximums close to the walls. This profile roughly models the current increase in shallow water close to land compared to more weaker currents at deeper depths in the middle. The current speed in the aperture was chosen to approximate the

modeled current in Moskstraumen. A maximum value of the current in Moskstraumen was estimated to be about 2–3 m/s (Gjevik et al., 1997) during one tidal cycle. We scaled the model so that the strength in the middle of the aperture (origin) was $v_0 = 1.5$ m/s in the y-direction which gave a maximum value of 2.5 m/s in the y-direction at the edges of the aperture ($\alpha = 6.6672 \times 10^{-5}$).

Steady BCs, with different magnitude and in opposite direction in the two regions, are superimposed on this flow. In regions 1 and 2, the BC are denoted, by $\vec{U}_1$ and $\vec{U}_2$, respectively. The BC are smoothed as tanh, this to avoid discontinuity in the aperture

$$\vec{U}_1 = |C_1| \tanh\left(\frac{y}{R}\right)\vec{i}, \quad \vec{U}_2 = -|C_2| \tanh\left(\frac{|y|}{R}\right)\vec{i}. \tag{7}$$

Here, C_1, C_2 are the strengths of the BCs and R the smoothing length. The vector $\vec{i}$ is the unit vector pointing in positive x-direction. Fig. 3 shows the current field with BC superimposed.

In Table 1, we have listed the essential fixed parameters and variables in this model. The variables, which will be studied more thoroughly are marked *var*. A function P of the variables
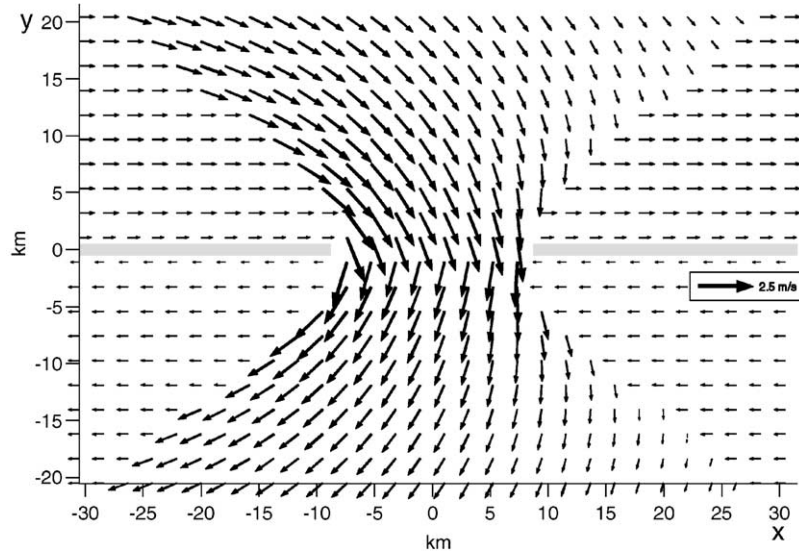
Fig. 3. Sketch of the idealized current field with the *BC* superimposed. In this figure, $C_1 = 0.7$, $C_2 = 0.5$, $t = 0$ and $\delta = 0$. We measure C_1, C_2 in m/s and t in seconds.

Table 1
Key parameters and variables for the idealized model

b	Width of the aperture	16 km
v_0	Strength of the current in origin	1.5 m/s
T	Period of the tide (M_2)	12.4 h
c	Foci of the hyperbolas	10 km
(x, y)	Location where particles are dropped	var
C_1	Strength of *BC* region 1	var
C_2	Strength of *BC* region 2	var
R	Smoothing length	var
δ	The phase of the oscillatory term	var

C_1, C_2, R, x and y, which measure the exchange of particles, can be defined as

$$P = \frac{\text{Number of particles changing region}}{\text{Total number of particles dropped in position } x, y}. \tag{8}$$

In the number of particles *changing region* in Eq. (8) only particles that leave their initial region permanently are counted. We here refer to P as the exchange parameter.

The exchange parameter P is a function of the variables C_1, C_2, R and y upstream in regions 1 and 2. As $|y|$ increases from the walls, P decreases

and will be zero for $y \geqslant L_1$ in region 1 and $|y| \geqslant L_2$ in region 2. P is a concave downward function of y. In a simulation of P, represented by Fig. 8, we estimate L_1 to be 8 km and L_2 to be 13 km. Altering C_1 and C_2 (0.1–0.7 m/s), the lengths L_1 and L_2 alter. If we keep $C_1 > C_2$, L_1 would change more than L_2. While L_2 would retain a value near 13 km, L_1 would change by several kilometers. By symmetry $L_1 = L_2$ for $C_1 = C_2$. If we alter the smoothing length R, we would also alter P. The intention of the smoothing length is only to avoid a discontinuity in the middle of the aperture. Keeping a reasonable size of R, we will generate a P with nearly same extension and distribution. For the simulations represented in this paper we have smoothed the *BC* by setting $R = 1$ km.

4.1. Results from the idealized model

The numerical time step, particle trajectories, particles released from a source, cluster simulations and estimation of the exchange parameter P (Eq. (8)) will be studied and represented in this section.

In Figs. 4 and 5, we demonstrate the importance of choosing an appropriate time step for the
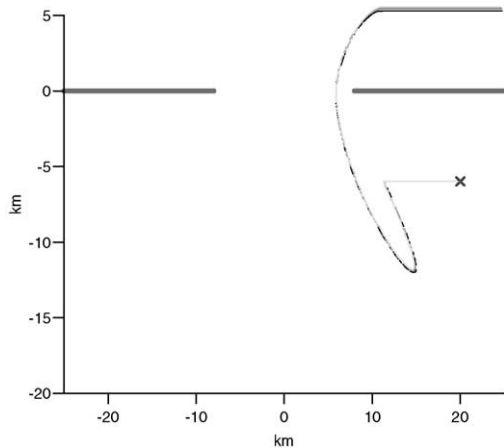
Fig. 4. Convergence of particle trajectory for a nonsensitive particle. Six particles are released under identical conditions, dropped in position $(20, -6)$ with different time step ($\Delta t = 0.105, 0.085, 0.065, 0.045, 0.025$ and 0.005 h) used in the numerical integration. In this figure, all six trajectories are indistinguishable. The total simulation time for each trajectory is within 29.17 ± 0.14 h. In this figure, $C_1 = 0.5$, $C_2 = 0.2$, $t_0 = 0$ and $\delta = 0$, see model description in Section 4.

idealized model. The position of initial release for the particles is marked by a $\times$. Particles were divided into two categories, sensitive and non-sensitive, according to their reaction of decreasing/increasing the numerical time step. Fig. 4 shows a nonsensitive particle, which has reliable trajectories even for "large" time steps. Fig. 5 shows a sensitive particle. For the sensitive particle it is crucial to integrate with a small time step. Nonsensitive particles are characterized by stability to perturbation in the phase $\delta \pm \Delta\delta$ of the current field or equivalent perturbation in the initial time of release $t_0 \pm \Delta t_0$. This means that for the particle in Fig. 4, released in the current field with a perturbation in phase, the particle would still leave through the aperture and remain on this new side for the rest of the simulation. Sensitive particles, however, are restricted to this small area spanned by the perturbations $[\delta - \Delta\delta, \delta + \Delta\delta]$ (or equivalent $[t_0 - \Delta t_0), t_0 + \Delta t_0]$). In this area, in the phase domain or time domain, we will have both particles that remain in their initial region and those who change region (see Fig. 2). The phase δ and the time t_0 in these expressions are not independent of the position of release (the particles

in Figs. 4 and 5 are released in the same position). In order to obtain a high degree of accuracy in the entire field we used a small time step set by the accuracy of the sensitive particles. This involves rather ineffective integration of the nonsensitive particles but sufficient integration for sensitive particles. However, the chosen time step did not increase the computational cost to an unacceptable level.

For the numerical simulations in this idealized model, a time step $\Delta t = 0.025$ h was used to ensure reliable trajectories of the particles released. If not elsewhere mentioned the particles are released at simulation start $t = 0$.

4.2. Particle trajectories

The current field is completely periodical and particles released on the same spot separated by the tidal period T will therefore have identical trajectories. For particles released within this period the trajectories can differ greatly.

In Fig. 6, six particles are released on the same spot uniformly separated by only $T/200$ h. The first three particles will remain in their initial region, while the last three change region. The figure shows that particles changing region do not necessarily leave through the aperture within the first outgoing current, that the trajectories of each particle is unique and that the time spent within the time-dependent current differs greatly.

4.3. Particles released from a source

The simulation in Fig. 6 can be regarded as a source releasing six particles uniformly during a time interval of 0.31 h. Here, we will extend this interval and study the patterns of the particles released from this source. A total number of 2000 particles are released over a time interval of 100 h, each separated by 0.05 h. Fig. 7 shows the result in this case.

Particles leaving the time-dependent current will build up patterns, like the loops in region 1 and the strings in region 2. The six particles shown in Fig. 6 capture the switch between particles that will build up strings (remain in their initial region)
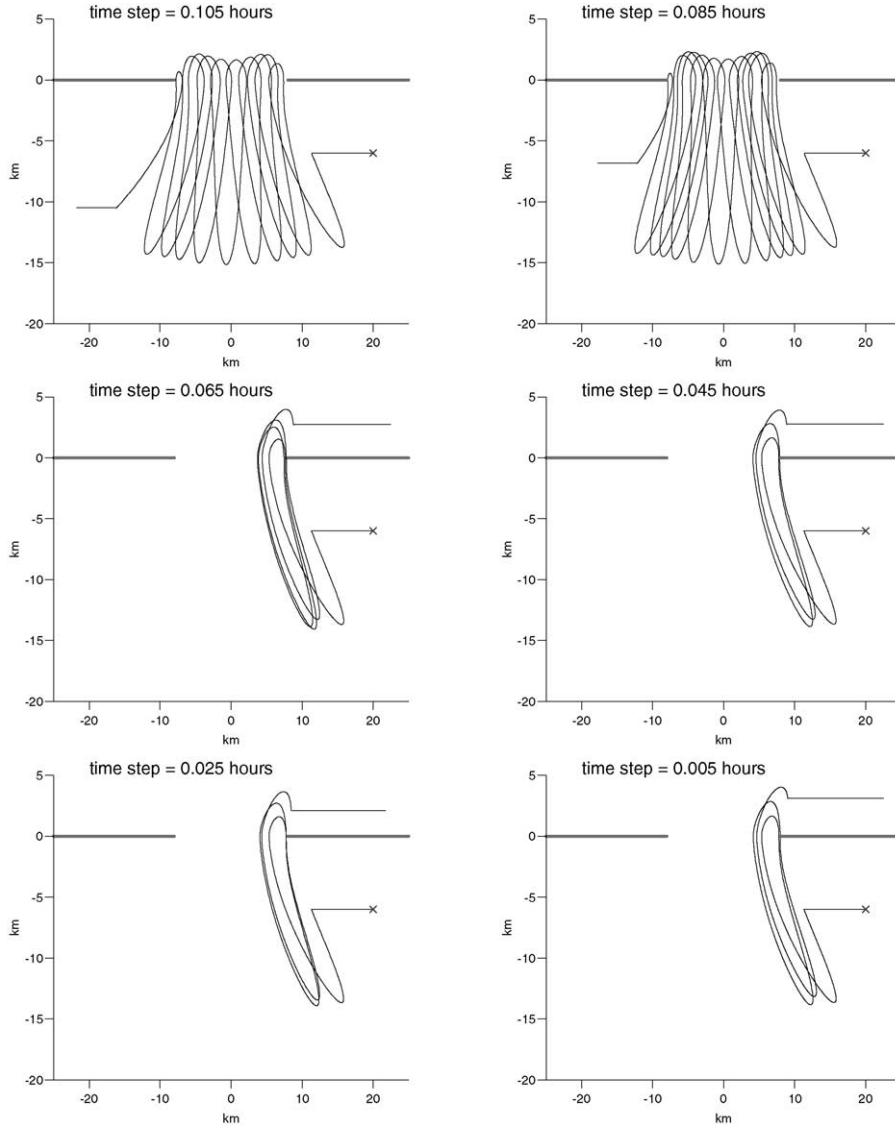
Fig. 5. Convergence of particle trajectory for a sensitive particle dropped in position $(20, -6)$. The particle is released under identical conditions and the particle trajectory is calculated with decreasing numerical time step Δt. The total simulation time varies from $55.95 (\Delta t = 0.025)$ to $169.66 (\Delta t = 0.085)$ h. In these figures $C_1 = 0.5$, $C_2 = 0.2$, $t_0 = 0$ and $\delta = 16.8\pi/100$, see model description in Section 4.

and those that will build up loops (changing region). The particle distribution in each loop (and in each string) will be identical if the separation time between each particle released from the source is proportional to the period T and if we wait until a steady state is obtained. During the simulation no two particles will enter the flow through the aperture under the same conditions, hence each particle has unique trajectories. If particles were released every T/M hour (M = number of particles), particles separated by the period T will follow the same trajectories.
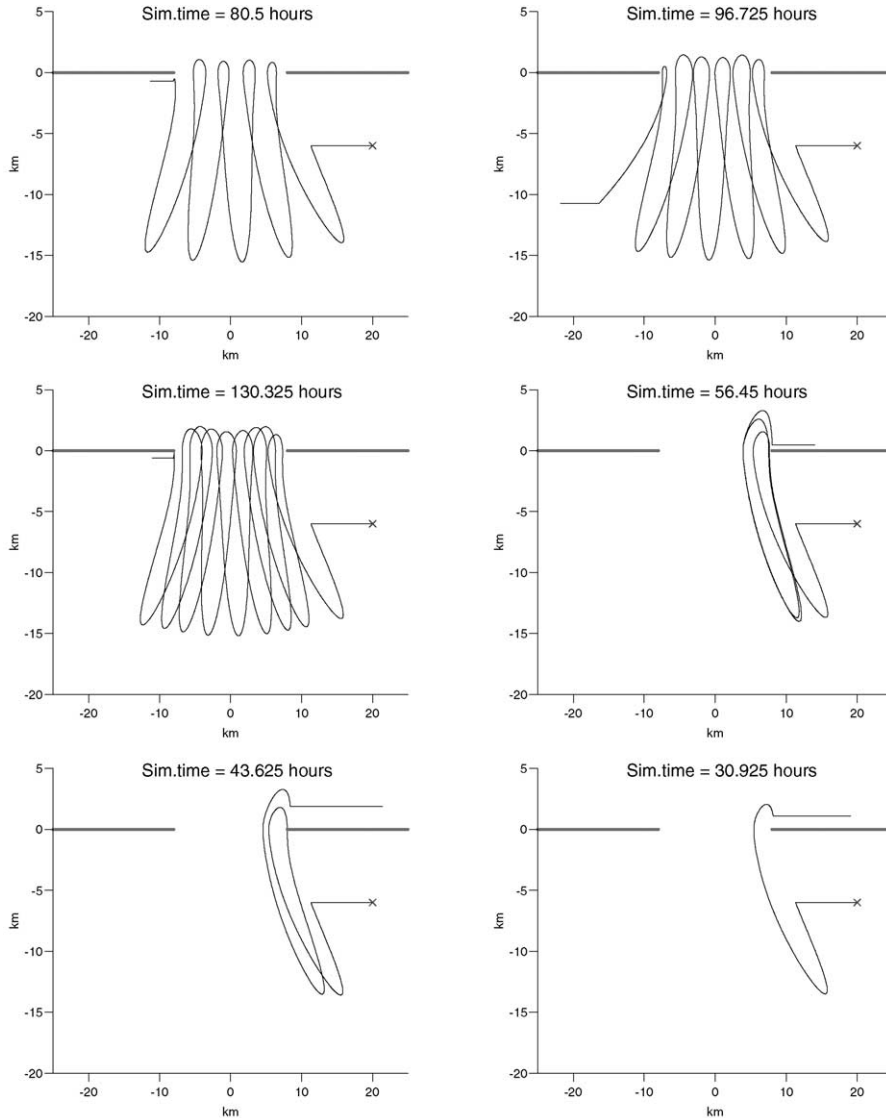
Fig. 6. The particles are released in coordinate $(20, -6)$. The phase δ is $\pi/5$, $C_1 = 0.5$, $C_2 = 0.2$ and the particles are released at, respectively, $t = 0, T/200, 2T/200, \ldots, (5T)/200$ h ordered left–right top–bottom. Each simulation is stopped 7.5 h after the particle leaves the time-dependent current. The time spent within the time-dependent current equals the simulation time (Sim.time) subtracted 19.525 h.

These particles leaving the time-dependent current will therefore build up identical clusters, separated by the length $|\vec{U}_1| \cdot T$ and $|\vec{U}_2| \cdot T$ in regions 1 and 2, respectively. Most of the particles in these clusters can be traced to particles released from the source within the same period. However, some particles can remain in the time-dependent current

for quite some time, as seen e.g. in Fig. 6 left middle panel. Such particles will therefore leave the time-dependent current together with particles descended from a later release. Steady state in this context is therefore obtained when all the particles from the first period have left the time-dependent current.
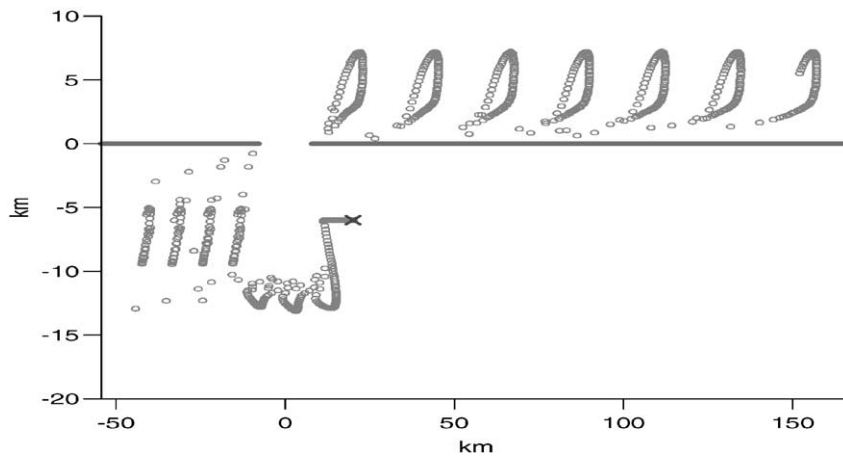
Fig. 7. 2000 particles (circles) released, each with 0.05 h separation, from a source located in coordinate $(20, -6)$. The phase δ is 0, $C_1 = 0.5$, $C_2 = 0.2$. Total simulated time is 100 h.
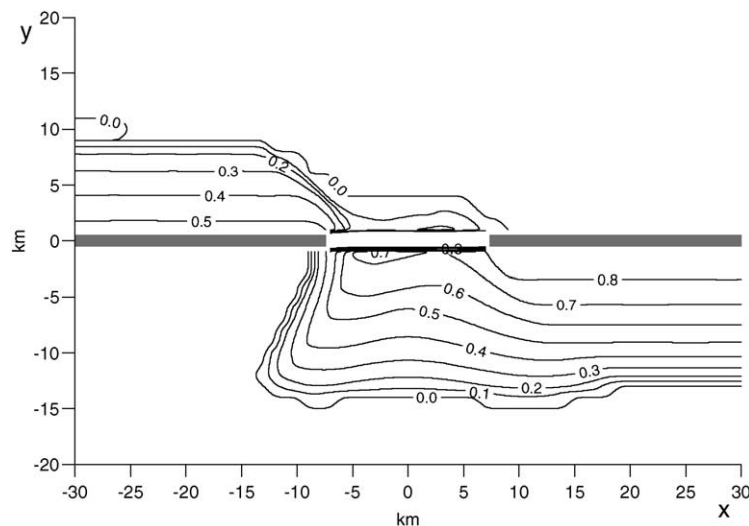

Fig. 8. Contour lines for the exchange parameter P with 0.2 separation near the aperture for $C_1 = 0.5$, $C_2 = 0.2$ (idealized model). Note, P is not defined for $y = 0$.

4.4. Cluster release and estimation of the exchange parameter P

A cluster of particles with an idealistic shape is released. The cluster consists of 5649 particles, separated by 0.1 km in the x-direction and 0.5 km in the y-direction, and has the shape of a square with upper left corner in coordinate $(20, -1)$ and lower right corner in $(48, -11)$. In this simulation,

the phase δ is 0, $C_1 = 0.5$, $C_2 = 0.2$. Simulation of 300 h drift ensured that all particles had left the time-dependent current. At end time we found 1916 particles in region 2 and 3733 in region 1.

In Fig. 8, we have depicted the exchange parameter P for the region near the aperture. The exchange parameter is calculated with a spatial resolution of 500 m. In each calculation point a total of 995 particles were uniformly

released during a time interval $2T$. The exchange parameter will be independent of the initial state of flow if we release many particles during a time interval $T_{sim} \gg T$ or if we release many particles during whole periods of T.

We can use the exchange parameter to predict the transport of a cluster. For example, the described square-cluster can be represented as fictitious sources along a line in the y-direction from coordinate $(20, -1)$ to coordinate $(20, -11)$ each releasing $5649/11 = 269$ particles during two tidal cycles. If we estimate P to be a linear function of y using just the values of P shown in Fig. 8 from coordinates $(20, -1)$ and $(20, -11)$, 3630 particles of the cluster were predicted to change region. An improved result was obtained by using the resolution of P from Fig. 8 along a line in the y-direction from coordinate $(20, -1)$ till coordinate $(20, -11)$. The amount of particles changing region with this technique was estimated to be 3727.

The ideal shape of the cluster ensures the good estimate. The cluster can be easily represented by sources releasing particles during a time interval $2T$. The amount of particles released from each of the fictive sources is multiplied by an estimate of P for the same position, and by addition of this value from all the sources representing the cluster we obtained the prediction represented. This technique gives good estimates for clusters which can be represented by s sources releasing over hole tidal periods or over time intervals $T_s \gg T$. These restrictions are necessary to ensure that the transport is not too heavily dependent on the initial state of the flow.

5. A realistic model

The Norwegian directorate of fisheries studied the amount of eggs and spawn in the North-Norwegian coastal waters during spring 1950 and 1951. Fig. 9 shows the distribution of cod eggs during spring 1951, taken from Wiborg (1952). We believe that most of the eggs found on the outer shelf descend from the most significant spawning area located in the northwestern part of Vestfjorden. However, Wiborg kept the possibility that the cod also has major spawning-areas on the outer

shelf. He doubted that a significant amount of eggs was transported from Vestfjorden to the banks outside Lofoten. We will study the trajectories from particles released in Vestfjorden to see whether a large amount of cod eggs on the outer shelf may descend from spawning in Vestfjorden.

The numerical tracking algorithm for this region is named *the Lofoten model* to make a distinction from the idealized model. The time step used in these simulations was found by investigating several paths from particles released in different position and in different times. The time step used, $\Delta t = 0.0125$ h, was then chosen by the most sensitive particle, see the discussion in Section 4.1. Section 5.1 shows particles which are transported only due to the periodical tidal current. In Section 5.2, a BC is added to simulate the general circulation. Section 6 shows the effect of the random-walk method.

5.1. Trajectories of single particles

The trajectories of particles released in Mosk-straumen will be sensitive to their initial time and position of release. Identical trajectories from particles released at the same spot in different times are naturally found separated by the tidal period T.

An anti-clockwise rotation of the current-vector is dominant in Vestfjorden, while on the outer shelf the rotation is dominantly clockwise. In the areas with weak current fields, we will have locale elliptic motions of particle; anti-clockwise in Vestfjorden and clockwise on the outer shelf. In Fig. 10, we have depicted the rotation and the tidal ellipses which show the strength of the current field. Measurements obtained in the G1 cruise April-77 (University of Bergen, Geophysical Institute) show an anti-clockwise rotation of the current-vector in stations S1 and S2 (depicted in Fig. 10) and clockwise rotation in stations S3 and S4. Our numerical tidal model is in good agreement with these measurements for the stations S1, S3 and S4 (Moe et al., accepted for publication). The station S2 is barely located inside the area with clockwise rotation in our model.

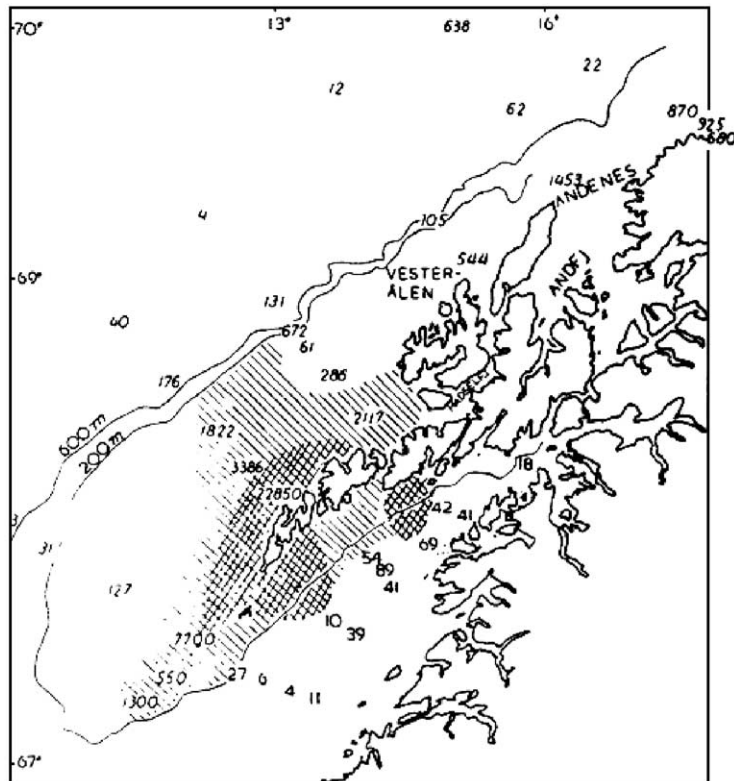Figs. 11–13 show a selection of some typical trajectories from particles released between

Fig. 9. Distribution of cod eggs in Lofoten 4–5 April 1951. Cross hatched: 1000–6000 eggs/m^2 Hatched: 100–1000 eggs/m^2. After Wiborg (1952).

Lofotodden and the island Værøy. Single particles were released at $t = 0$ and 60 h drift was simulated. The left panel of Fig. 11 shows one particle with local elliptic motion, released at distance and west of Mosken. The particle is released in an area where there is only small gradients in the current field. The clockwise motion agrees well with the rotation of the current vector depicted in Fig. 10. The right panel demonstrates beaching of a single particle. The particle was beached after 27.74 h and will remain on the small islands Mosken. Fig. 12 shows the oscillatory nature of the flow. The particle in left panel shows typical local oscillatory, while the oscillation of the particle on right panel is not restricted to such a small area. Fig. 13 illustrates the sensitivity of drop-position and the forcing of complex topography. The left panel shows a particle that loops around Mosken.

The drop position is changed by 100 m in the x-direction for the particle on the right panel.

The particle trajectories show that the tidal excursion of Moskstraumen is capable of transporting eggs and spawns from Vestfjorden to the outer shelf. The strong current is restricted to a thin band from Værøy to Lofotodden. Typical trajectories are: local elliptic motion outside this band and more complex oscillatory motion from particles released inside. Eggs and spawns from the north-west part of Vestfjorden must therefore be transported close to the tip of Lofotodden if Moskstraumen is able to capture them.

5.2. Motion of a cluster of particles

A cluster of particles was released in a region near Lofotodden. Fig. 14 left panel shows the

initial position of this cluster, which is made up of 313 particles, shaped in a circle with radius 2 km.

The drifting cluster is captured by Moskstraumen, and Fig. 15 shows the position of each
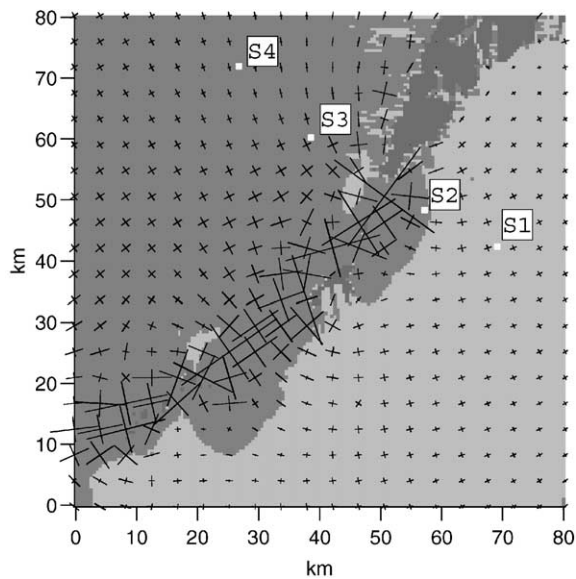

Fig. 10. The rotation of the current vector. Bright shadowing depicts region with anti-clockwise rotation, darker shadowing depicts region with clockwise rotation. The crosses show the major and minor axis with a reduced resolution to avoid cluttering. The eccentricity calculated for this area ranges from 0.23 to 1.0 with common values near 1. Areas with low eccentricity is found near Værøy and Røst (Røst is the island located near coordinate (20,20). Location of the measurements from the G1 cruise depicted by S1–S4.

particle after 6, 12, 18 and 24 h. Only five particles were beached after 24 h, of which three were beached at the small island Sørholmen (coordinate 14.5, 19) and two at the island Rødøy (coordinate 15.5, 18). Rødøy is merged with Lofotodden due to the grid resolution used here. We increased the simulation time to ensure that a majority of the cluster did not experience a "mathematical beach". Fig. 14 right panel shows the end position of this cluster after 100 h. Moskstraumen has dispersed this cluster. The current field forced by the small island Mosken will contribute strongly in this dispersion. Of the total 313 particles released 10 beached near Lofotodden and 32 at Mosken. Moskstraumen transports a large part of the cluster in between the inner and outer shelf, and the cluster is strongly stretched and reshaped. The mechanism is the same as in the idealized model, a periodical current. The complex drift of particles released, illustrated by Figs. 11–15 is due to gradients in the Eulerian current field. We also placed the initial cluster 4 km further east, in this case no particles would enter the outer shelf and the cluster would move in an elliptic motion and still be cluster-shaped after 100 h simulation (plots not shown here). Furthermore, the cluster (Fig. 14 left panel) was also released at other stages of the tide. This naturally changes the trajectories for the individual particles but the general movement of the cluster will still resemble the drift shown in Figs. 14 and 15.
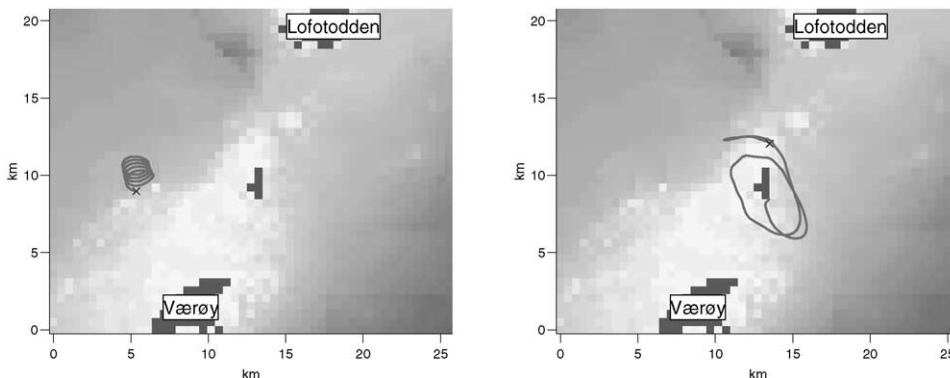

Fig. 11. Left panel: particle released in coordinate (5.5, 9) demonstrates typical local elliptic motion in distance from the small island Mosken (located in the middle of Lofotodden and Værøy). Right panel: particle released in coordinate (13.5, 12) shows the deadlocking, beaching of particles that enters a dry grid.
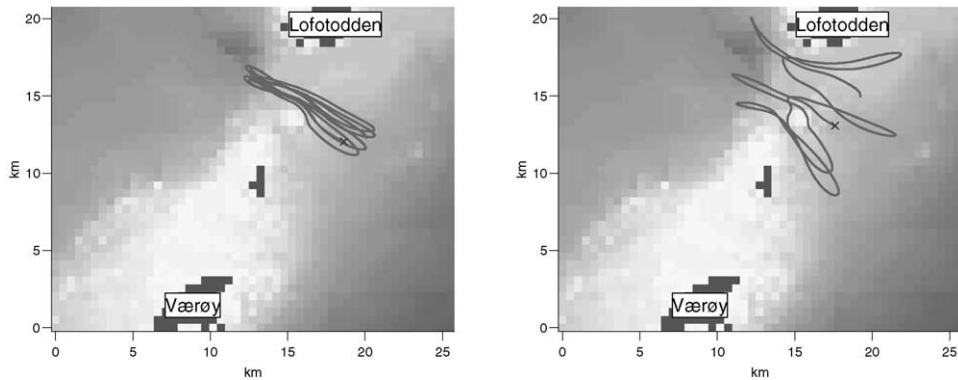
Fig. 12. Left panel: particle released in coordinate (18.5, 12) shows local oscillatory motion. Right panel: particle released in coordinate (17.5, 13) shows oscillatory motion with more complex trajectory.
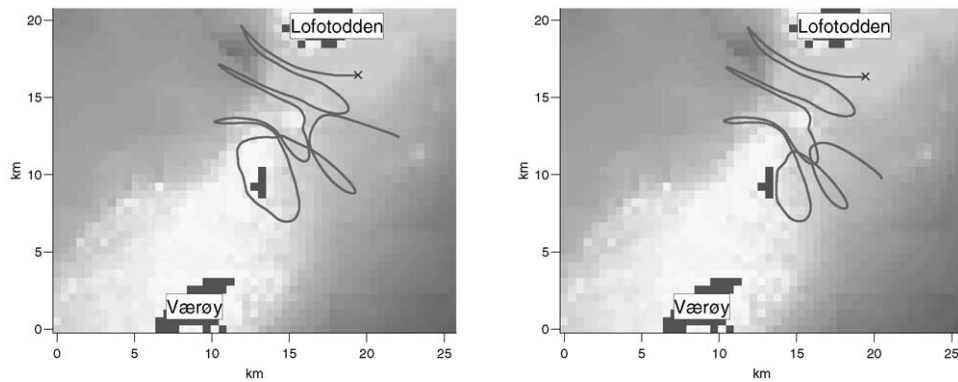

Fig. 13. Left panel: particle released in coordinate (19.3, 16.2). Right panel: particle released in coordinate (19.3, 16.3). The particles demonstrate forcing of topography and the sensitivity in drop position.
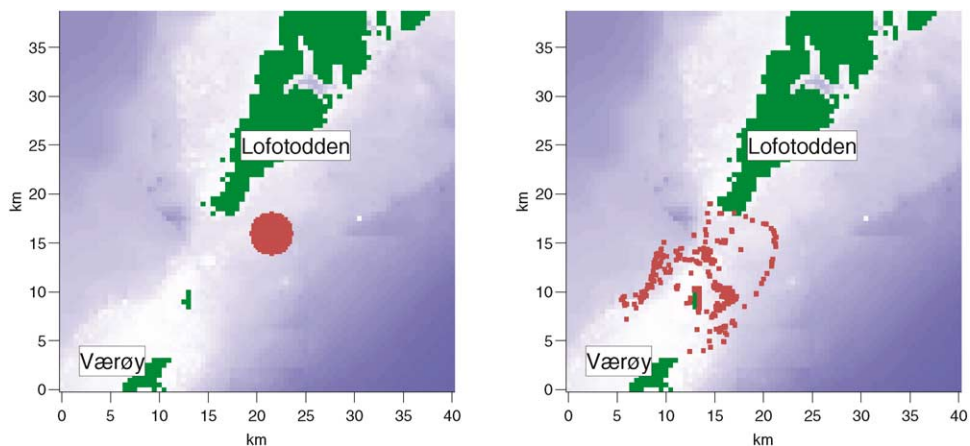

Fig. 14. Left panel: initial drop position of a circular cluster made up by 313 particles with a radius of 2 km. The center of the cluster is located in coordinate (21.5, 16.5). Right panel: end position of particles after 100 h drift in the tide.
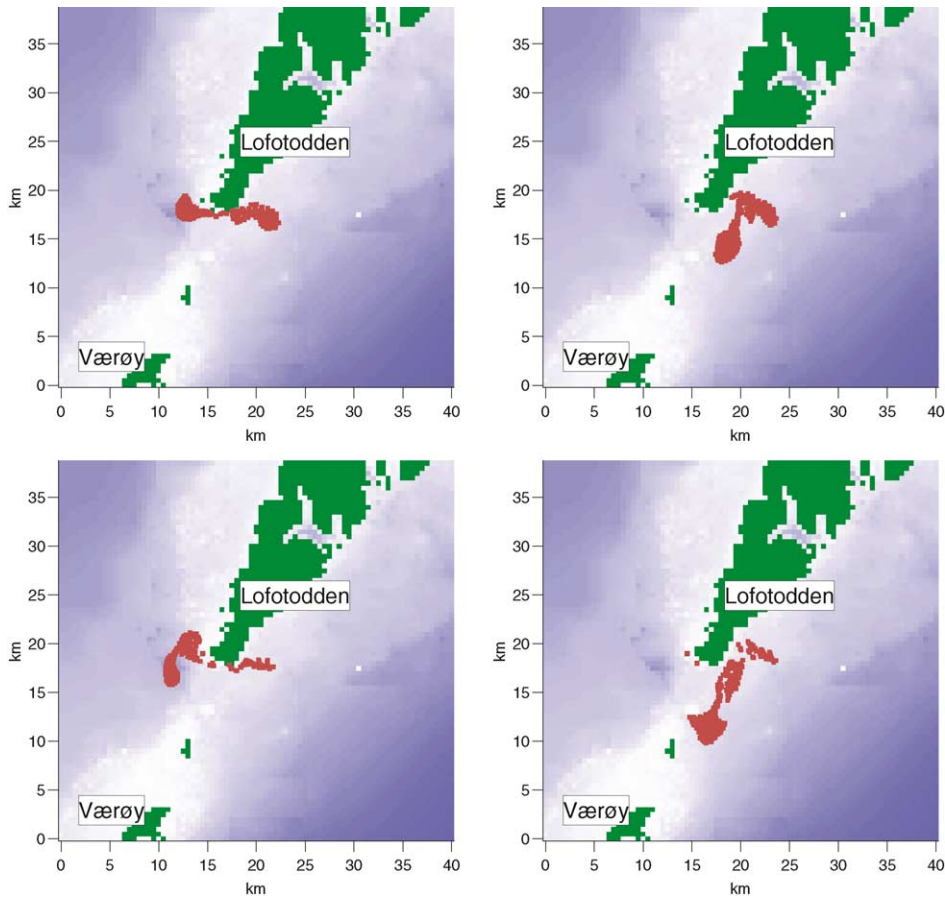
Fig. 15. Drift and dispersion of the cluster are due to the tide. The simulated drift is for 6, 12 (upper panels), 18 and 24 h (lower panels).

5.3. Effect of background current (BC)

We have designed idealized BC in order to simulate the general circulation introduced by the Norwegian Coastal Current in the area. One branch of this coastal current enters Vestfjorden on the south-east side and exits along the Lofoten archipelago on the west side, Furnes and Sundby (1980). In this section, we will study drift of particles with additional BC. We simply add to the oscillatory tidal current a constant northward shelf current on the west side of the Lofoten island and a constant southward current inside the Lofoten islands. Fig. 16 indicates the location and the separation zone between the two branches of the

steady current. If not elsewhere mentioned we have used a constant northward depth mean current of 0.3 m/s and a constant southward depth mean current of 0.1 m/s.

The addition of BC will dramatically alter the trajectories of particles released. To avoid steady drift towards or from islands and land BCs were only added two grid-points from dry points (zero depth).

5.4. Particle trajectories

Fig. 17 shows two typical trajectories of single particles. The particle on the left panel is captured

by Moskstraumen and transported towards the northward *BC*. Although being trapped in the strong current for several periods, the particle never enters the northward *BC*. On the right panel we have released a particle at the same spot, but with a delay of 0.1 h. This particle enters the northward *BC* and is transported northward. These two particles demonstrate the change in particle trajectories due to a short phase distur-bance. Picture a source placed at coordinate $(25.5, 23)$, the first particle is one of the last

particles that will leave south-east of Værøy, while the second particle is one of the first particles entering the outer shelf during the first tidal period. The same situation is depicted for the idealized model in Fig. 6.

In our model, eggs found on the outer shelf can only descend from Vestfjorden if they once were transported close to the tip of Lofotodden. For this particular run the crucial border is within approximately 5 km east of the tip of Lofotodden (Fig. 18). This result is strongly dependent on our choice of *BC*. We calculated the exchange para-meter for different *BC* strengths and defined the beach parameter to be

$$B = \frac{\text{Number of particles beached}}{\text{Total number of particles dropped in position } x, y}.$$

(9)

The beach parameter is defined to quantify the amount of beached particles and to ensure reliability in the representation of *P*. The beached particles were counted as particles unable to change region. The effect of increasing/decreasing the northward *BC* (within 0.2–0.5 m/s) does not alter much the shape and extension of the exchange parameter shown in Fig. 18. Increasing the southward *BC* gives a more linear *P*, with $P = 0$ at approximately $x = 24$ km.

During these simulations, with the simplified *BC* and without diffusion, there is a possibility for
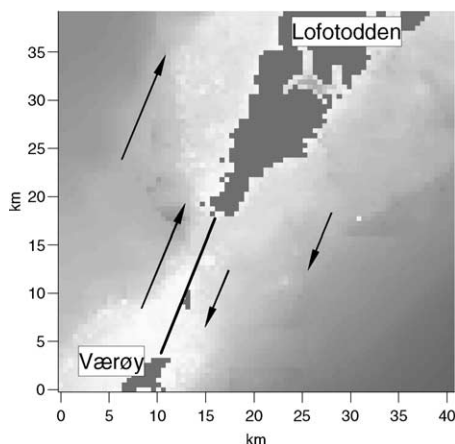

Fig. 16. The structure of the idealized *BC*s. The arrows show the current direction, and the solid line the separation zone between the two branches of the current.
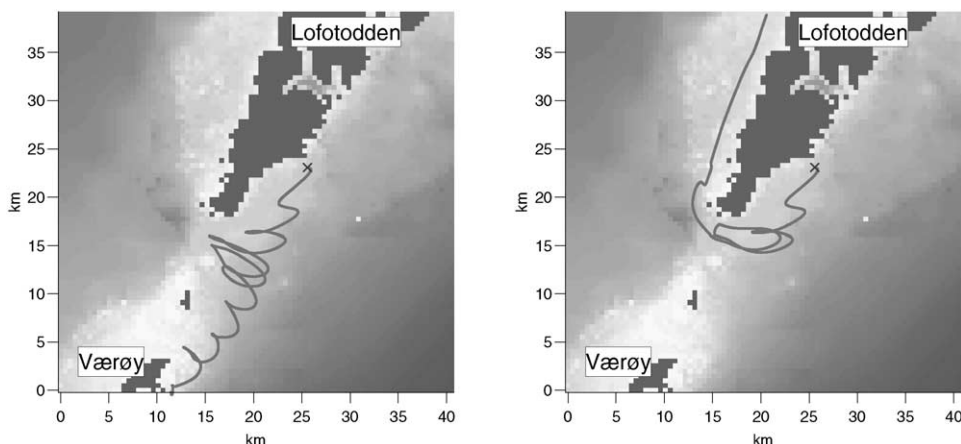

Fig. 17. Two particles released in coordinate $(25.5, 23)$, separated by 0.1 h. Left panel: particle released at $t = 7.1$ h with 122.9 h drift. Right panel: particle released at $t = 7.2$ h with 60 h drift.

particles to be trapped within Moskstraumen. From Fig. 18, and other simulations of P and B, beaching was only considered a problem when particles were released very close to land ($x \approx 18.5$)

5.5. Motion of a cluster of particles

Fig. 19 is one example of drift and dispersion of a cluster with BC. The initial position, shape and size of the cluster are as described and illustrated in Fig. 14 left panel. In this simulation beaching of particles is not considered a problem. After 24 h only 12 particles beached. They were all found deadlocked on the island Sørholmen. A great amount of particles are transported in a northward direction in this simulation. Approximately, 30% of the cluster is transported through the sound between Mosken and Lofotodden and transported in a

northward direction already after 12 h. Moskstraumen transports the particles in between Vestfjorden and the outer shelf and many particles are captured by the northward BC. Of the total 313 particles released in Vestfjorden, 244 permanently changed region and 57 left the model domain southward on the inner shelf (the remaining 12 were beached).

6. Diffusion simulated by random walk

The random-walk approach enables simulation of diffusion processes without solving the advection diffusion equation. We used the random-walk method mainly to simulate small scale homogeneous turbulence, although several other options are possible. The results presented here are with a constant diffusion coefficient, but simulations were also made where the strength of the diffusion was related to the eddy viscosity (current shear) or to the tidal speed.

The random-walk method alone performed, according to the analytical results presented in Section 3, as a generator of the Fickian diffusion with an effective diffusivity coefficient $K \approx K_h$. An increase in the amount of particles released will improve the performance of the random-walk method as a simulator of diffusion, see e.g. Furnes (1994) and/or Hunter (1980). This improvement will naturally increase the computational cost.

We used the fourth-order Runge–Kutta method for the numerical integration of Eq. (3). The random-walk method displaces each particle to a length D at each time step, so we can no longer use a multistep method (Adams–Moulton).

Fig. 20 shows a repitition of the simulation in Section 5.3 now with the random walk method included to simulate small scale turbulence. As expected horizontal small scale turbulence will smear out the cluster shapes but the general drift pattern is preserved, as seen from Figs. 19 and 20. A moderate diffusion coefficient has been used to demonstrate the effect of the random-walk method. More data on the strength of the small scale turbulence are needed to construct a more realistic diffusion coefficient.
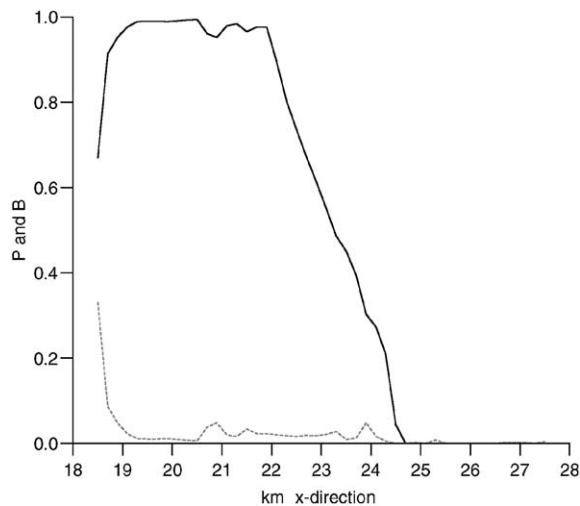

Fig. 18. The exchange parameter calculated along a line from coordinate (18.5, 18.25) to (28, 18.25) with the sources separated by 200 m. 1000 particles were uniformly released by each source during a time interval equal to the tidal period. The simulation of the particles was stopped when all particles had either *changed region*, beached or left south-east of Værøy. The dotted line shows B defined in Eq. (9) for the same area. Since most of the beached particles will be sticking to the tip of Lofoten (the separation zone) they are counted as particles that do not change region. The particles being transported southeast of Værøy are stopped, so the fact that particles may also enter the outer shelf south of Værøy is not considered.
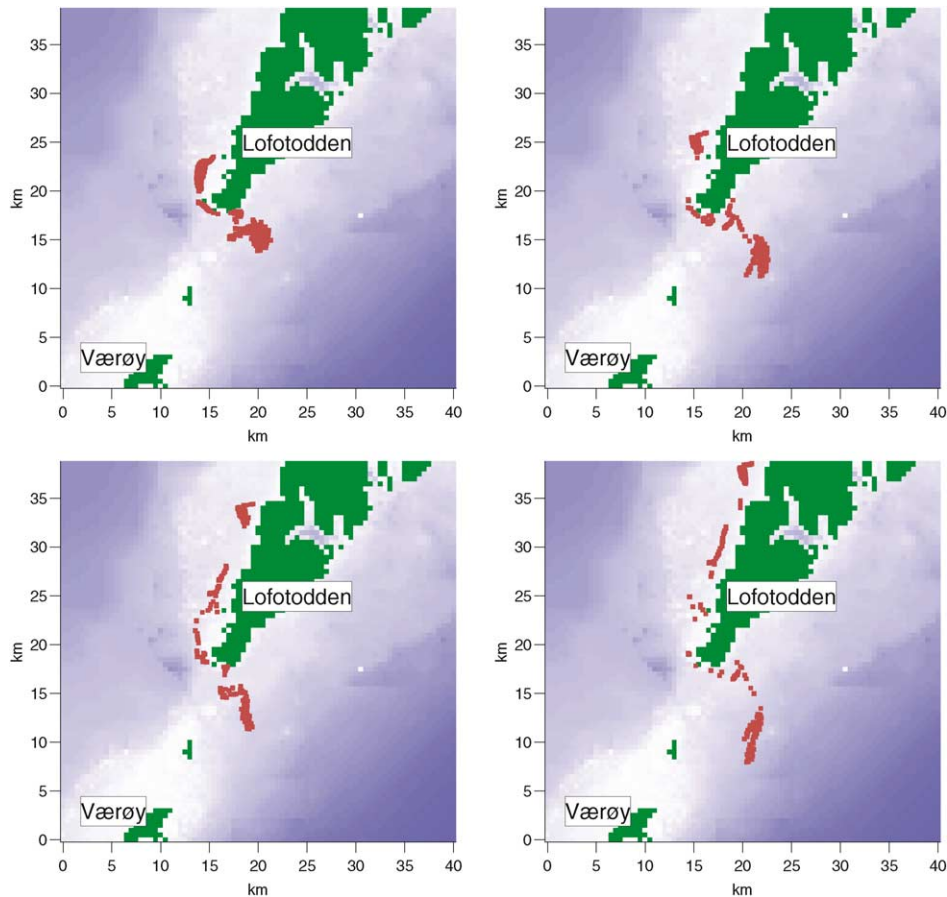
Fig. 19. Drift and dispersion of the cluster with the addition of *BC*. The initial position of the cluster is shown in Fig. 14 left panel. The simulated drift is for 6, 12 (upper panels), 18 and 24 h (lower panels).

7. Concluding remarks

A particle tracking algorithm is implemented for the Lofoten region. Trajectories are computed from data obtained by a harmonic analysis of the current times series modeled in Gjevik et al. (1997). The tracking of particles from Vestfjorden demonstrates that the tidal current in Moskstraumen combined with the steady *BC*s in this region is an important mechanism for the water exchange between Vestfjorden and the outer shelf. This mechanism may explain why a large amount of cod eggs in some cases are found on the outer shelf, despite the fact that the important spawning area is located inside Vestfjorden, close to the Lofoten archipelago.

An idealized model was developed to demonstrate the exchange mechanism. This idealized model was used to demonstrate the importance of finding a suitable time step for the numerical integration. The idealized model represents the current profile in Moskstraumen, and it is justified through the simulations. To quantify the exchange an *Exchange Parameter*, measuring the water exchange in different positions, was constructed.

With our constructed *BC* in the Lofoten model the eggs found on the outer shelf, which initially descend from Vestfjorden, must once have been
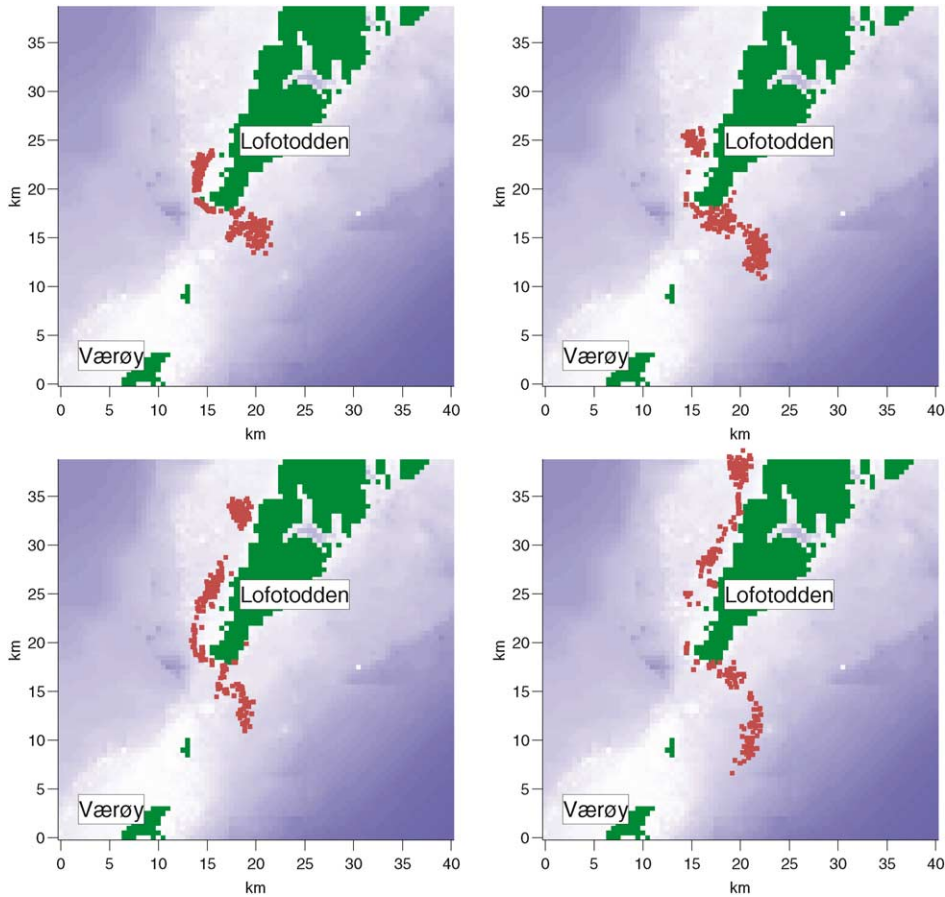
Fig. 20. Drift and dispersion of the cluster with the addition of *BC* and diffusion. The simulated drift is for 6, 12 (upper panels), 18 and 24 h (lower panels). The diffusion coefficient K_h is 10 m^2/s.

transported by the *BC* within approximately 5 km east of Lofotodden. This is to enable the tidal excursion in Moskstraumen to transport them into the northward directed current. Within this 5 km border the *Exchange Parameter* revealed that the likelihood for a particle leaving for the outer shelf may be as large as one, and such a large exchange may exist within a large part of the border. Unfortunately, there seem to be no field experiments with drifters in this area to verify these model predictions.

In this model, Moskstraumen is considered the only outlet between Vestfjorden and the outer shelf. Other outlets, like south of Værøy and the straits in the northern part of the Lofoten

archipelago, are also important for the water exchange between Vestfjorden and the open sea. A similar mechanism for water exchange (tidal current combined with *BC*) will also occur in these regions. Since the other straits in the northern part are long and narrow and combined with an expected reduction in tidal excursion the pumping of the tide will be less efficient compared to that in Moskstraumen. More realistic modeling of the *BC* are needed to quantify this exchange.

We deadlock particles when they encountered the extension of a dry grid point (zero depth). The contour of the grid point was not considered and current shifts could not transport the particles back into the simulation. Beaching was only

considered a problem in the calculation of P when the calculation point was within one grid cell distance from Lofotodden. With our treatment of beached particles, we decided to add BC only in a distance of two grid points from dry grid points. This is to prevent steady drift from or towards land.

We implemented a random-walk method to simulate small scale turbulent diffusion. This is an effective and computationally cheap approach. The method is well known for modeling a diffusion process, but like in the advection–diffusion equation its correctness is strongly dependent on the use of an appropriate diffusion coefficient model.

Our basic tidal model neglects the effect of dispersion due to residual currents. A nonlinear (3D) model and better knowledge about BC are necessary to make more accurate and reliable estimates of the particle trajectories. In our model, the periodic nature of the tidal current enables a study of particle trajectories from only a small initial data subset. Expanding the model with nonlinear terms leads to different and tougher computation of trajectories. The particle tracking algorithm must then be implemented together with the nonlinear model. Particles initial positions and time of release must be pre-declared, and this will most likely lead to a computationally costly nonlinear model being recalculated several times. The complexity and chaos of the trajectories may even force a smaller time step in the nonlinear model.

Trajectories from particles released in Mosk-straumen were very site and time dependent, and the tidal current field alone lead to strong dispersion of clusters released due to the strong gradients in the current field. An approach using the theory from chaotic motion (Hamilton) for this region was made, but the divergence of the current field combined with limiting the scope of this paper suggested this topic as a prospective future study.

Acknowledgements

References

Boyce, W.E., DiPrima, R.C., 1992. Elementary Differential Equations and Boundary Value Problems, 5th Edition. Wiley, New York.

Ellertsen, B., Furnes, G.K., Solemdal, P., Sunby, S., 1980. Influence of wind induced currents on the distribution of cod eggs and zooplankton in Vestfjorden. In: Sætre, R., Mork, M. (Eds.), The Norwegian Coastal Current, Vol. 2 of Proceedings from the Norwegian Coastal Current Sympo-sium, Geilo, University of Bergen, pp. 604–628.

Elliott, A.J., 1986. Shear diffusion and the spread of oil in the surface layers of the North Sea. Deutche hydrographische Zeitscrift 39, 113–137.

Elliott, A.J., Dale, A.C., Proctor, R., 1992. Modelling the movement of pollutants in the UK Shelf Seas. Marine Pollution Bulletin 24 (12), 614–619.

Elliott, A.J., Hurford, N., Penn, C.J., 1986. Shear diffusion and the spreading of oil slicks. Marine Pollution Bulletin 17 (7), 308–313.

Furnes, G.K., 1994. Discharges of produced water from production platforms in the North Sea. Technical Report R-064641, Norsk Hydro.

Furnes, G.K., Sundby, S., 1980. Upwelling and wind induced circulation in Vestfjorden. In: Sætre. R., Mork, M. (Eds.), The Norwegian Coastal Current, Proceedings from the Norwegian Coastal Current Symposium, Geilo, Vol. 1, University of Bergen, pp. 152–177.

Geyer, W.R., Signell, R.P., 1992. A reassessment of the role of tidal dispersion in estuaries and bays. Estuaries 15 (2), 97–108.

Gjevik, B., 1996. Models of drift and dispersion in tidal flows. In: Grue, J., Gjevik, B., Weber, J.E. (Eds.), Waves and Nonlinear Processes in Hydrodynamics. Kluwer Academic Publishers, Dordrecht, pp. 343–354.

Gjevik, B., Moe, H., Ommundsen, A., 1997. Sources of the Maelstrom. Nature 388 (28), 837–838.

Hunter, J.R., 1980. An interactive computer model of oil slick motion. Oceanology International 80, 42–50.

Hunter, J.R., 1987. The application of Lagrangian particle-tracking techniques to modelling of dispertion in the sea. In: Noye, J. (Ed.), Numerical Modelling: Application to Marine Systems. Elsevier, Amsterdam, pp. 257–269.

Milne-Thomson, L.M., 1968. Theoretical Hydrodynamics, 5th Edition. Macmillan, New York.

Moe, H., Ommundsen, A., Gjevik, B. A high resolution tidal model for the area around The Lofoten Islands, Northern Norway. Preprint Series, Department of Mathematics,

University of Oslo. Submitted to Continental Shelf Research, accepted for publication.

Proctor, R., Elliott, A.J., Flather, R.A., 1994a. Forecast and hindcast simulations of the Braer oil spill. Marine Pollution Bulletin 28 (4), 219–229.

Proctor, R., Flather, R.A., Elliott, A.J., 1994b. Modelling tides and surface drift in the Arabian Gulf—application to the Gulf oil spill. Continental Shelf Research 14 (5), 531–545.

Ridderinkhof, H., Zimmerman, J.T.F., 1992. Chaotic stirring in a tidal system. Science 258 (13/11), 1107–1111.

Turell, W.R., 1994. Modelling the Brær oil spill—a retrospective view. Marine Pollution Bulletin 28 (4), 211–218.

Wiborg, K.F., 1952. Forekomst av Egg og Yngel i Nordnorske Kyst- og Bankfarvann Våren 1959 og 1951. Fiskeridirektorates Småskrifter 1, 1–22.

Zimmerman, J.T.F., 1986. The tidal whirlpool: a review of horizontal dispersion by tidal and residual currents.. Netherlands Journal of Sea Research 20 (2/3), 133–154.